Temperature and magnetic field-dependent x-ray powder diffraction study of dysprosium

A. S. Chernyshov,[1,2,*] Ya. Mudryk,[2] V. K. Pecharsky,[1,2,†] and K. A. Gschneidner, Jr.[1,2]
[1]*Department of Materials Science and Engineering, Iowa State University, Ames, Iowa 50011-2300, USA*
[2]*Ames Laboratory, Iowa State University, Ames, Iowa 50011-3020, USA*
(Received 29 November 2007; published 26 March 2008)

An x-ray powder diffraction study of polycrystalline Dy was performed over the temperature interval from 5 to 300 K in applied magnetic fields up to 40 kOe. A complex first-order magnetostructural transformation, which occurs below ~8 kOe and above ~20 kOe, is decoupled into a first-order magnetic (helix-fan) transition and a second-order magnetostructural (hexagonal-orthorhombic) transition between ~135 and ~175 K in magnetic fields between ~8 and ~20 kOe. The transition to the ferromagnetic (FM) state is always accompanied by an orthorhombic distortion of the hexagonal lattice, including a transition from the paramagnetic (PM) to the FM state in magnetic fields exceeding 20 kOe.

DOI: 10.1103/PhysRevB.77.094132 PACS number(s): 61.50.Ks, 71.20.Eh, 81.30.Hd, 81.30.Bx

INTRODUCTION

The rare-earth metal Dy has been broadly studied over the last few decades due to its interesting magnetism, which includes high magnetocrystalline anisotropy, large localized magnetic moment ($p_{\text{eff}}=10.65\mu_B$), and complex magnetic structure.[1] At room temperature, Dy is paramagnetic (PM). On cooling in a zero magnetic field, a helix antiferromagnetic (AFM) ordering occurs at $T_N=180$ K (Néel point), followed by a transformation to the ferromagnetic (FM) structure when the temperature is below $T_C=90$ K (Curie point). The latter occurs via a coupled magnetostructural transition.[2–5] At temperatures ranging from the Curie point to 135 K, an applied magnetic field transforms the magnetic structure directly from a helix to a ferromagnetic type, whereas between 135 K and the Néel point, the AFM-FM transition is separated by an intermediate fan magnetic phase stable in the range of magnetic fields from ~7 to ~25 kOe.[6,7]

According to low temperature x-ray diffraction studies of Dy single crystal, its hexagonal close packed (hcp) crystal structure observed at room temperature distorts orthorhombically at the Curie point in a zero magnetic field with pronounced discontinuities in lattice parameters.[2,3,5] At T_N, no sharp changes were observed but the strong expansion of the c parameter below 180 K was reported.[2,3,5] The single crystal x-ray diffraction investigation of Dy in low magnetic fields ($H\leq 1$ kOe) was carried out in the vicinities of both the Curie and Néel temperatures.[5] The presence of a narrow (4 K wide) region where the AFM and FM phases coexist was postulated from splitting of the (006) Bragg peak into two components: hexagonal AFM and orthorhombic FM. The same study[5] reported the temperature dependencies of the lattice parameters in low magnetic fields near the critical points and showed that magnetic field applied along the easy magnetization direction (a axis) shifts the kink in the c-lattice parameter associated with T_N. Contrary to the reported magnetic-field–temperature (H-T) phase diagram,[6,8,9] the kink moves to higher temperatures at an anomalously high rate of ~8 K/kOe.[5] This observation was not supported by the linear thermal expansion (LTE) measurements along different crystallographic axes in a Dy single crystal in applied magnetic fields up to 14 kOe.[10] A single crystal investigation[11] reported temperature and magnetic field dependencies of the c-lattice parameter in magnetic fields up to 60 kOe. A sharp increase was observed at 130 and 150 K in 8 and 10 kOe fields, respectively, whereas at 170 K, a relatively smooth kink was detected around 10 kOe. An x-ray powder diffraction investigation of polycrystalline Dy at 77, 145, and 300 K in applied magnetic fields up to 13.8 kOe notes a hexagonal to orthorhombic distortion during isothermal magnetization at 145 K accompanied by a steplike change of the c-lattice parameter.[12] Correlations between commensurability points, where the magnetic helix structure becomes commensurate with the crystal structure, and anomalies in thermal expansion were reported by Greenough *et al.*[13]

Upon ordering, the magnetic moments of Dy atoms lie in the basal ab plane (Fig. 1) of the hexagonal close packed structure.[1] Thus, in the magnetically ordered state Dy has ferromagnetically ordered planes stacked along the c axis. The Ruderman-Kittel-Kasuya-Yoshida (RKKY) interactions have oscillating character strongly dependent on the interatomic distances. Therefore, the magnetic structure is sensitive to magnetic field and temperature dependencies of the c-lattice parameter. This is why all previous examinations of the crystal structure in applied magnetic field were concerned

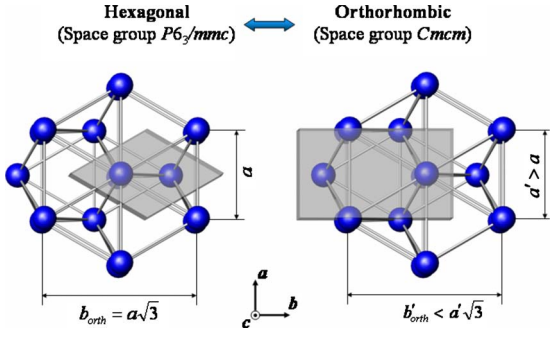

FIG. 1. (Color online) A comparison of the hexagonal ($T=290$ K, $H=0$) and the orthorhombic ($T=60$ K, $H=0$) unit cells of dysprosium. The gray rhombus and the gray rectangle represent the basal planes of the unit cells of these two structures.

with the measurements of the *c*-lattice parameter, even though the hexagonal-orthorhombic transformation is a distortion of the hexagonal networks in the basal *ab* plane.

There are a number of papers where the magnetic phase diagram of Dy was constructed using different experimental techniques. These include bulk magnetization,[4,14] magnetocaloric effect,[8] Young's modulus,[9] ultrasonic measurements,[15] and calorimetry.[16] Our recent work[7] presented a detailed investigation of a dysprosium single crystal that combined dc magnetization, ac magnetic susceptibility, heat capacity, and direct measurements of the magnetocaloric effect. The magnetic phase diagram with the magnetic field vector along the easy magnetization *a* axis was refined, and several new anomalies were reported. A nearly temperature independent first order transformation was observed around the T_C=90 K from heat capacity measurements in applied magnetic fields up to 20 kOe. Additional anomalies were reported near the commensurability point at 113 K. A phenomenological model based on Landau-Ginsburg theory was proposed to explain the observed anomalies. The model considers the existence of spiral antiferromagnetic clusters consisting of six pairs of *ab* planes, each with mutually opposite magnetic moments. Heat capacity measurements of Ref. 7 confirmed the observations of Refs. 11 and 16 that the fan phase splits into two regions in the magnetic *H-T* phase diagram: the low-temperature region between 135 and 165 K (fan I) and the high-temperature region that spans from 165 K toT_N=180 K (fan II). The fan phase is a special case of a helical magnetic structure, in which direction of magnetic moments of the ferromagnetic *ab* planes not only varies periodically along the *c* axis, but the moments are constrained to lie within a certain interval of angles (fan angle sector) usually locked close to the direction of the magnetic field. The microscopic description of the fan phases, as well as neutron scattering experiments which confirm the difference between fan I and fan II, may be found in Refs. 1, 17, and 18.

Here, we present a detailed x-ray powder diffraction study of polycrystalline Dy over the temperature interval 5–300 K in applied magnetic fields up to 40 kOe. The objective of this work is to directly investigate structural changes in polycrystalline Dy and correlate them with the observed complex behavior of thermal (heat capacity) and magnetic properties (magnetization and magnetocaloric effect) of Dy.

EXPERIMENTAL DETAILS

The polycrystalline Dy investigated in this work was prepared by the Materials Preparation Center at the Ames Laboratory.[19] The major impurities in the metal were as follows (in ppm atomic): O-600, C-190, F-110, Fe-60, N-50, and the total of all other impurities was ~50 ppm atomic. Thus, the starting material was 99.89 at. % (99.98 wt. %) pure. Dysprosium powder was prepared by sanding a piece of metal using an 80 grit Al_2O_3 sand paper. Even though Dy is paramagnetic at room temperature, its particles are attracted to a high-power Neomax-type permanent magnet due to the high magnetic moment of the dysprosium atom. Thus, we used magnetic separation to clean Dy powder from the nonmagnetic Al_2O_3 dust. After pulverizing and cleaning, the powder was screened through a 75 μm sieve, wrapped in a Ta foil, sealed in a quartz tube, and annealed for 3 h at 400 °C to relieve strains produced in a sample during sanding. A piece of Dy metal was placed in the same quartz tube to getter residual oxygen and reduce oxidation of the powder during the heat treatment. The final product contained about 10 wt. % total of two (predominantly surface) oxides Dy_2O_3 [oxide A: CaF_2 type, space group $Fm3m$, Dy in 4(a), 100% occupation, and O in 8(c), 75% occupation, a=5.2127(4) Å; and oxide B: Mn_2O_3 type, space group $Ia\bar{3}$, a=10.669(3) Å], as determined from x-ray diffraction measurements at room temperature. This is due to the surface oxidation that occurred during grinding as well as during the heat treatment of the powder.

The powder was mounted on a copper sample holder, filling a $24.5\times21.4\times0.5$ mm^3 cavity and thoroughly mixed with a diluted by methanol GE varnish. After drying and baking at 120 °C for one hour, a flat surface was formed by using a 380 grit sand paper to improve resolution of powder diffraction patterns. The x-ray powder diffraction data were collected on a Rigaku TTRAX rotating anode powder diffractometer with Mo $K\alpha$ radiation in the Bragg angle interval ranging from 2θ=11° to 2θ=55°. The sample temperature was controlled within ±0.02 K below 50 K and better than ±0.05 K above 50 K using a continuous helium flow cryostat. A split-coil superconducting magnet was used to create magnetic fields ranging from 0 to 40 kOe; the field vector was coplanar with the plane of the specimen.[20]

Multiple sets of diffraction patterns were collected in a step scanning mode with 0.01° steps of 2θ and counting time 1 s/step. Each pattern was refined using EXPGUI-GSAS (Refs. 21 and 22) to determine the positional parameters of the individual atoms (for the orthorhombic phase) and the unit cell dimensions. Profile residuals (R_p) were from 6 to 8 % and derived Bragg residuals were from 3 to 5 %. Preferred orientation in the hexagonal phase of Dy (space group $P6_3/mmc$) was accounted using spherical harmonic approximation (cylindrical symmetry, eighth order, six independent parameters) implemented in GSAS.[21] The texture index was 1.29. The same coefficients obtained during the refinement of the hexagonal phase were used for the refinements of the orthorhombic phase. Additional free variables in the spherical harmonic approximation of texture, which appear due to the lower symmetry of *Cmcm* space group compared to $P6_3/mcm$, were constrained to zero.

RESULTS

At room temperature, dysprosium adopts the hcp structure (space group $P6_3/mmc$). Figure 1 shows the basal plane projected along the *c* axis of the room-temperature hcp and low-temperature orthorhombic crystal structures of Dy. The gray rhombus and the rectangle represent the basal planes of the unit cells of these two structures.

Geometrically, the hexagonal structure can be also described as an orthorhombic one with the lattice parameters $a_{orth}=a_{hex}$, $b_{orth}=a_{hex}\sqrt{3}$, and $c_{orth}=c_{hex}$. After cooling dysprosium below $T_C\approx90$ K, the basal plane of the hexagonal

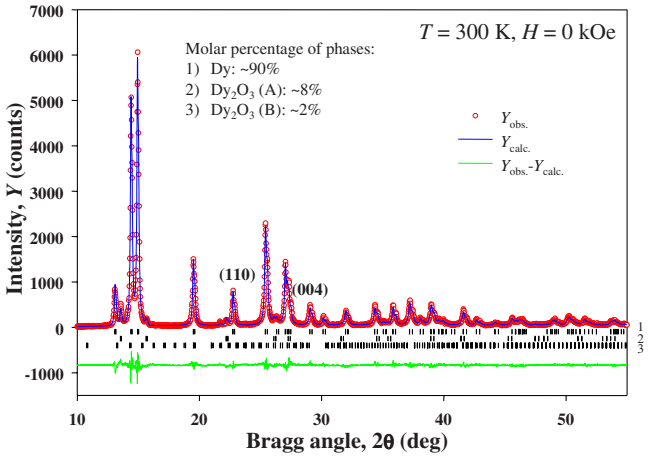

FIG. 2. (Color online) The x-ray powder diffraction pattern of Dy collected in a zero magnetic field at 300 K. The profile residual (R_p) was 6% and derived Bragg residual (R_B, for hcp Dy) was 5%. The uppermost set of the vertical bars located just below the pattern indicates calculated positions of Bragg peaks for both $K_{\alpha 1}$ and $K_{\alpha 2}$ components of hcp Dy and the sets below represents the same for Dy_2O_3 phases (A in the middle and B at the bottom). The Bragg reflections (110) (basal plane) and (004) (c axis) are marked.

structure distorts, and the actual lattice parameter b_{orth} deviates from an ideal $a\sqrt{3}$ value (see Fig. 1). This distortion results in a structural transformation from hcp-Dy to its orthorhombic polymorph.

The x-ray powder diffraction pattern of polycrystalline Dy collected at 300 K and subjected to the Rietveld refinement is shown in Fig. 2. To illustrate structural changes, two representative Bragg reflections, the (110) and (004), may be used. Since the orthorhombic distortion occurs in the basal (ab) plane, the splitting of the (hh0) peak is an indicator of the distortion in the hexagonal plane. Despite the fact that the splitting is more pronounced at higher Bragg angles (higher values of h), the (110) reflection has a relatively high intensity. The shift of the (004) peak position is a good indicator of changes along the c axis.

Figures 3 and 4 show the temperature dependencies of Bragg intensity recorded on heating of the sample from 20 to 140 K in the vicinities of these two reflections. The contour maps represent patterns collected at different temperatures with a step of 5–10 K; the dashed lines follow the intensity maxima corresponding to the $K\alpha_1$ components of the Bragg peaks in the patterns. The splitting of the hexagonal (110) peak into orthorhombic (200) and (130) peaks and the shift of the (004) peak at temperatures around 90 K are seen.

The temperature dependencies of the a-lattice parameter of dysprosium in a zero magnetic field are presented in Fig. 5(a). While cooling, the a-lattice parameter of the hcp structure splits into a- and $b/\sqrt{3}$ orthorhombic parameters around 90 K due to the orthorhombic distortion, as was reported by Refs. 3 and 12. The temperatures of transformations on heating and cooling are ~95 and ~80 K, respectively (taken at the maximum $|\Delta a/a|$). Thus, the specimen exhibits a significant hysteresis (~15 K), which serves as additional evidence of the first order transformation. A large hysteresis between heating and cooling is typical for powders in comparison to

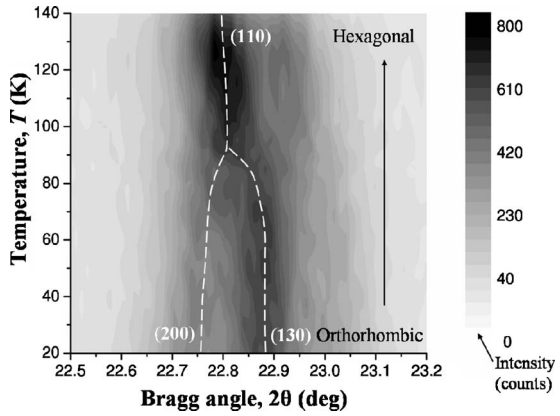

FIG. 3. The contour map of Bragg intensity in the vicinity of the hexagonal (110) peak and orthorhombic (200) and (130) peaks recorded on heating from 20 to 140 K. The dashed lines follow maxima of intensity corresponding to the $K_{\alpha 1}$ components of the Bragg peaks.

bulk samples and, particularly, single crystals. Two phases coexist both on cooling and heating over a ~10 K wide region, which is also larger than the same observed in a single crystal, where phase coexistence region was only ~4 K.[5] The temperature dependencies of the c parameter [Fig. 5(b)] show similar values of the transition temperatures and temperature hysteresis, even though the discontinuity is less obvious during heating. The observed expansion of the c-axis below T_N agrees with the previously reported results.[2,3,5,11] The disagreement between the heating and cooling curves above the T_N is within experimental errors and no thermal hysteresis is seen at the Néel temperature.

The temperature dependencies of the a-lattice parameter (hexagonal structure) and a and $b/\sqrt{3}$ parameters (orthorhombic structure) on heating in applied magnetic fields 3, 12, and 30 kOe are presented in Fig. 6(a), and the 7, 12, and 20 kOe magnetic field temperature dependencies of the a-lattice parameter on heating (both hexagonal and orthorhombic) are reported in Fig. 7. The curves exhibit a struc-

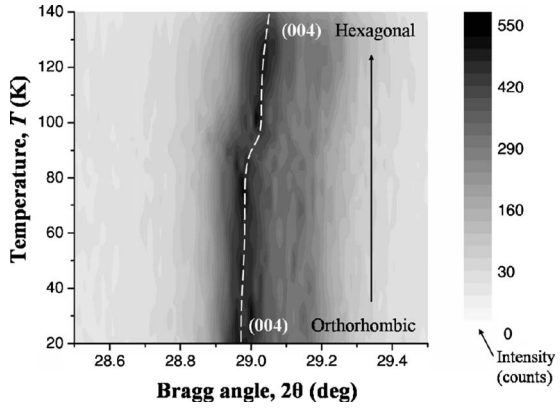

FIG. 4. The contour map of Bragg intensity in the vicinity of the (004) peak recorded on heating from 20 to 140 K. The dashed line follows the maximum of intensity corresponding to the $K_{\alpha 1}$ component of the Bragg peak.

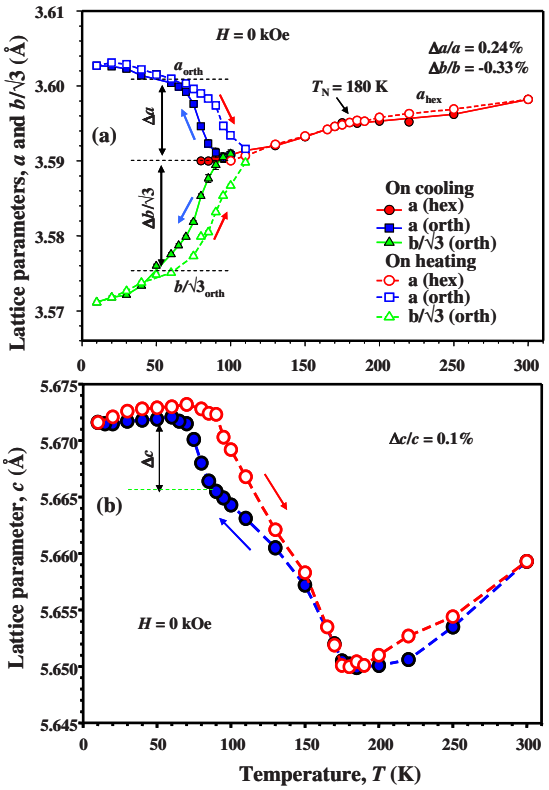

FIG. 5. (Color online) (a) Temperature dependencies of the hcp a and of the orthorhombic a and $b/\sqrt{3}$ lattice parameters and (b) the c-lattice parameter of dysprosium on heating and cooling in a zero magnetic field between 5 and 300 K.

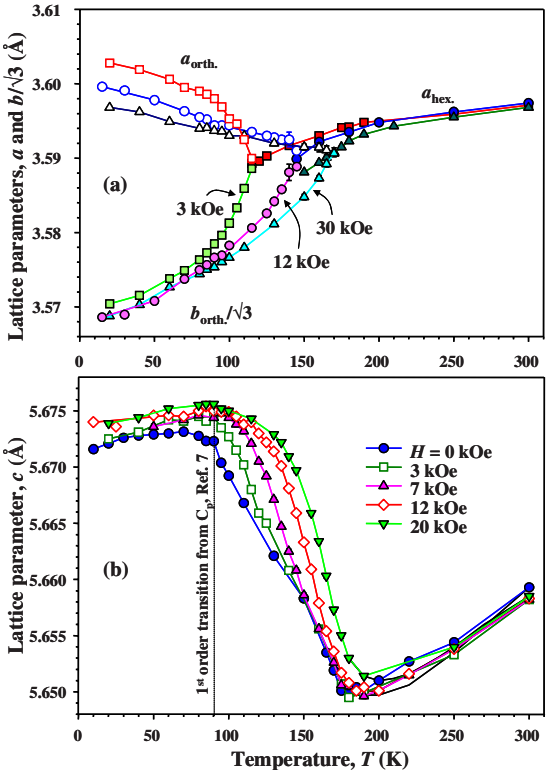

FIG. 6. (Color online) (a) Temperature dependencies of the hcp a and of the orthorhombic a and $b/\sqrt{3}$ lattice parameters recorded on heating in the temperature interval 5–300 K, obtained in constant magnetic fields of 3, 12, and 30 kOe. (b) The temperature dependencies of the c-lattice parameter in 0, 3, 7, 12, and 20 kOe magnetic fields recorded on heating in fixed magnetic fields. The vertical line indicates the broad maxima on the temperature dependencies of c-lattice parameter.

tural transition from the hexagonal to the orthorhombic structure type that shifts from 115 K (H=3 kOe) to 145 and 165 K in 12 and 30 kOe magnetic fields, respectively [Fig. 6(a)]. These values are in good agreement with the LTE measurements in applied magnetic fields reported by Clark *et al.*[10] Sharp singularities between 130 and 165 K (Fig. 7), depending on the magnetic field, correspond to the structural transition. Weaker, kinklike anomalies are also observed around 90 K in all curves (these are marked by arrows in Fig. 7).

Figure 6(b) shows the temperature dependencies of the c-lattice parameter in applied magnetic fields up to 20 kOe. All the curves have a minimum around 180 K that corresponds to the Néel point. A broad maximum around 90 K shifts little, if any, in applied magnetic fields exceeding 3 kOe.

The isotherms representing field dependencies of basal plane lattice parameters for hexagonal and orthorhombic structures in the range of magnetic fields 0–40 kOe are presented in Fig. 8(a). The curves were collected when increasing the magnetic field at fixed temperatures after zero field cooling. The structural transformation occurs in 5, 9, and 18 kOe magnetic fields at 115, 135, and 155 K, respectively. Furthermore, there are changes of slope in a_{hex} at lower fields, which are marked by arrows and highlighted by a dashed line crossing the three sets of curves in Fig. 8(a).

The c-lattice parameter isotherms at 115, 135, 155, and 175 K have steps at 5, 7, 10, and 10 kOe magnetic fields,

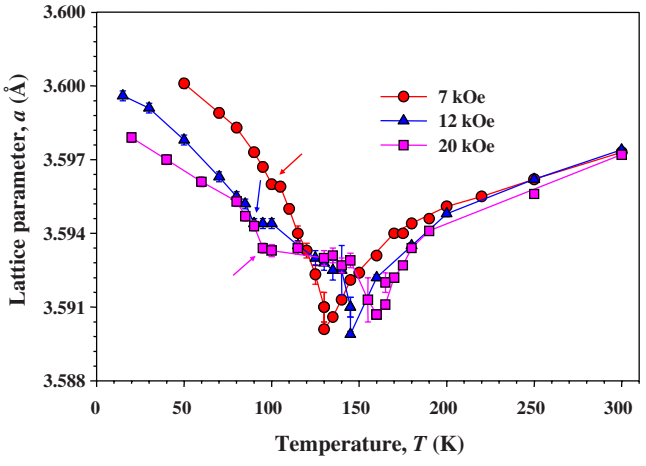

FIG. 7. (Color online) The temperature dependencies of the hcp and the orthorhombic a-lattice parameter in constant magnetic fields of 7, 12, and 20 kOe recorded on heating in the temperature interval 5–300 K. The arrows indicate the kinks on the curves at low temperatures (orthorhombic structure). The sharp minima correspond to the onset of the hcp-orthorhombic distortion.

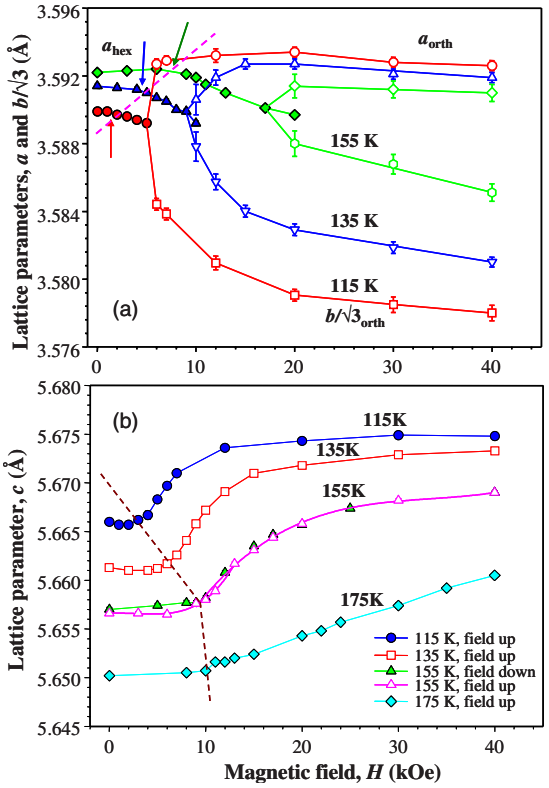

FIG. 8. (Color online) (a) The isotherms measured at 115, 135, and 155 K representing the hcp a (solid symbols) and the orthorhombic a and $b/\sqrt{3}$ lattice parameters (open symbols) as a function of magnetic field. The arrows indicate changes of slope, best seen on the 155 K isotherm. (b) The isotherms representing the c-lattice parameter at 115, 135, 155, and 175 K as a function of magnetic field.

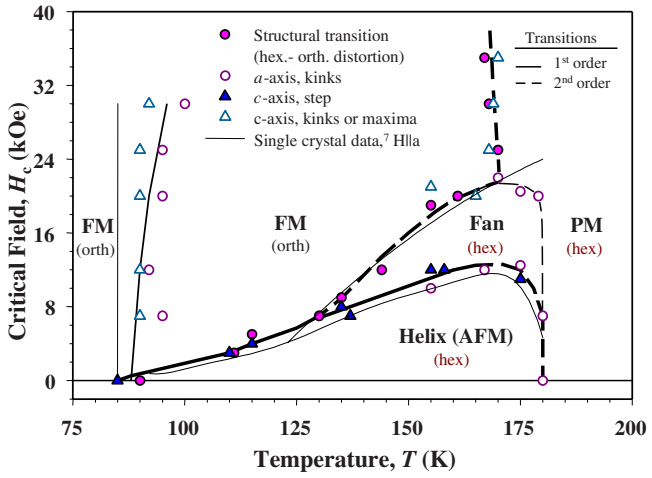

FIG. 9. (Color online) The structural H-T phase diagram of Dy polycrystal obtained from x-ray powder diffraction data compared to the magnetic phase diagram obtained from single crystal measurements of magnetization, heat capacity, and magnetocaloric effect (Ref. 7).

respectively [see Fig. 8(b)], in good agreement with Kida *et al.*[11] Obviously, the basal plane parameters and the c parameter behave differently during magnetization. For example, the hexagonal-orthorhombic structural transition [Fig. 8(a)] occurs at 155 K and 18 kOe with a kink at 10 kOe, whereas only the step in the c-lattice parameter at 155 K [see Fig. 8(b)] takes place at 10 kOe. Two isotherms at 155 K [see Figs. 8(a) and 8(b)] were measured, during magnetization and demagnetization, and they show little hysteresis during the low-field transition around 10 kOe and no hysteresis during hexagonal-orthorhombic transition at 18 kOe. When compared with the magnetic phase diagram,[7] it appears that low field anomalies correspond to the AFM-fan transition whereas the structural distortions coincide with the fan to FM transformation.

Figure 9 represents the structural H-T phase diagram of Dy constructed from analyses of basal plane and c-lattice parameters behavior described above. The solid circles interpolated by the bold lines, both solid and dashed, follow the boundary of the hexagonal-orthorhombic distortion [see Figs. 5(a), 6(a), 7, and 8(a)], whereas the solid triangles show the steplike anomalies of the c-lattice parameter [see Figs. 6(b) and 8(b)]. The open circles and triangles correspond to minor anomalies of lattice parameters, in Figs. 6(b), 7, and 8(a). The continuous lines in Fig. 9 correspond to the first order transitions, and the dashed lines correspond to the second order transitions. The thin lines representing magnetic phase boundaries are taken from Ref. 7, where a study of Dy single crystal with the magnetic field applied along the a axis was carried out using dc magnetization, ac susceptibility, heat capacity, and direct magnetocaloric effect measurements. Clearly, the magnetic phase diagram of Ref. 7 corresponds well to the structural H-T diagram derived from x-ray powder diffraction data though the former one was constructed by using single crystal data.

DISCUSSION

The x-ray powder diffraction measurements described above are in good agreement with previous magnetic,[4,6,7,14] thermal,[7–9,16] and structural[2,3,5,11,12] measurements of dysprosium. The structural H-T phase diagram is similar to the previously reported magnetic diagrams.[4,6,7,9,14,15] There is a correspondence between our results and data collected by using single crystal x-ray diffraction technique,[2,3,5,11] however, the intervals of the transitions are much broader in the case of polycrystalline Dy. The sharp steps in lattice parameters are hardly visible during the hexagonal-orthorhombic transition due to significant Bragg peak broadening and large thermal hysteresis. Thus the discontinuities of the lattice parameters were determined at the temperatures where the heating and cooling curves begin to coincide below the transition [marked by horizontal dashed lines in Fig. 5(a)], assuming that this is the end of the transition. The estimated changes of the lattice parameters at the Curie temperature are $\Delta a/a=0.24\%$, $\Delta b/b=-0.33\%$, in fair agreement with the $\Delta a/a=0.2\%$, $\Delta b/b=-0.5\%$ reported in Ref. 3. The change of the c-lattice parameter in a zero magnetic field [see Fig. 5(b)] is $\Delta c/c=0.1\%$, which is slightly lower than previously reported from x-ray measurements $\Delta c/c=0.2\%$ (Ref. 5) and $\Delta c/c=0.3\%$.[3] The results of LTE measurements in zero mag-

netic field are close to our values ($\Delta c/c=0.17\%$ and $\Delta a/a=0.27\%$).[10]

The broad Bragg peaks are the main reason why we did not observe really sharp discontinuities on the temperature dependencies of lattice parameters (see Figs. 5–8). In addition, it is possible that lattice parameters in the transition region are averaged as a result of Rietveld refinement due to phase coexistence. In these cases the nature of a transition (first order or second order) was assigned from the presence (or absence) of hysteresis and by a careful comparison with the heat-capacity data of Ref. 7.

The present investigation maps the intimate relationships between the magnetic and crystallographic transitions in Dy as seen in the combined field-temperature phase diagram (Fig. 9). The first-order AFM-FM transition occurs over the temperature interval 90–135 K in magnetic fields below 8 kOe. At higher temperatures the transformation to the FM state proceeds through an intermediate fan magnetic phase, which is stable over the temperature interval from 135 K to the Néel point (180 K) in the range of magnetic fields 8–22 kOe. Considering that the layered magnetic structure of Dy consists of ferromagnetically ordered planes stacked along the *c* axis, it is clear that the interplay between helix, fan, and FM phases is mostly determined by the interlayer distances (the *c*-lattice parameter) as follows from significant changes in the *c* parameter when the system undergoes any magnetic transformation (also see Ref. 11). Between 80 and 135 K the step along the *c* axis coincides with the hexagonal-orthorhombic distortion coupled with the AFM-FM magnetic transition (see Fig. 9). At temperatures above 135 K, the crystallographic and magnetic transitions split into the first order helix-fan transition with the related jump of the *c*-lattice parameter and the second order fan-FM transition, which is accompanied by the orthorhombic distortion. Hence, the helix-fan transition occurs without a change of the symmetry of the lattice; it only takes place with a step in the *c*-lattice parameter. The fan-FM transition can be also identified on the magnetic field dependencies of the *c* parameter by the change of slope,[11] but its most characteristic feature is the hexagonal-orthorhombic distortion. The important conclusion is that a transition to the FM state is always coupled with the orthorhombic distortion of the hexagonal lattice (see Fig. 9). So the minimum of free energy of the ferromagnetic phase is reached for the orthorhombic lattice, whereas all other magnetic structures exist in the hexagonal lattice.

According to magnetic measurements[4,7,8] and a single crystal x-ray diffraction study[11] the first order magnetic transformation from helix to FM and/or fan structure becomes second order at the so-called tricritical point at 170 K. Our measurements confirm the change of the order of the transition. Figure 8(b) shows that the magnetic-field-dependent isotherm of the *c*-lattice parameter at 175 K has only a change of slope instead of a characteristic discontinuous step, which is present at 115, 135, and 155 K. It is worth noting that the change of the order of the AFM-fan transition also affects the fan-FM (PM) transformation. According to our data (see Fig. 9), the fan-FM transition below the tricritical point occurs simultaneously with the orthorhombic distortion, whereas the fan-PM transition in the temperature interval from tricritical (170 K) to the Néel point occurs without any structural change. No obvious structural effects, which can be assigned to the fan-I–fan-II phase boundary,[14] have been observed. However, a difference in the behavior of the $T=175$ K isotherm compared with the other isotherms shown in Fig. 8(b) is consistent with the results of a crystallographic study of a single crystal,[11] and may be indicative of the fan-I (stable below 170 K) to fan-II transformation.

Recent measurements of heat capacity of a high-purity dysprosium single crystal revealed unusual anomalies in the vicinity of the Curie point in magnetic fields applied along the easy *a* axis. According to Chernyshov *et al.*,[7] a sharp peak observed at the Curie temperature (90 K) in a zero magnetic field, does not shift to higher temperatures when magnetic field increases despite the fact that the Curie temperature does.[4,6–8] However, an additional steplike anomaly appears in the heat capacity vs *T* curve in applied magnetic fields. When the magnetic field increases, this steplike feature quickly moves towards high temperatures following the AFM-FM transition boundary until the fan phase appears at $T=135$ K and $H=8$ kOe and then the anomaly follows the fan-FM transition boundary. This generally agrees with the x-ray powder diffraction data; one can see anomalies in the vicinity of Curie point marked by arrows on temperature dependencies of the *a*-lattice parameter (see Fig. 7). However, as we noted above, both the broad Bragg peaks and polycrystalline nature of the sample (Dy has a strong magnetocrystalline anisotropy) did not allow us to resolve the expected sharp discontinuities in the lattice parameters and unit-cell volumes. It is worth noting that a steplike anomaly of the heat capacity from Ref. 7 corresponds to the boundary of the hexagonal-orthorhombic transition, which also follows the fan-FM magnetic transition at temperatures above 135 K (see Fig. 9).

The origin of the large field-independent first-order type peak in heat-capacity measurements of Dy single crystal remains unclear. Obviously, in nonzero magnetic fields, it is no longer associated with the hexagonal to orthorhombic distortion, and yet no other orthorhombic to orthorhombic structural changes were detected. The structural effects around 90 K, which may be related to the field-independent heat-capacity peak, are detected by a broad maximum in the *c*-parameter dependences and kinks in the *a* parameter. However, these structural features appear too weak in order to cause such a large heat-capacity effect even assuming the difference between single-crystalline and polycrystalline samples and recalling a strong single ion anisotropy of the Dy^{3+} ion, and a strong dependence of the crystallographic response of the system on the orientation of the magnetic field vector with respect to crystal axes.[10] On the other hand, the polycrystalline nature of the sample enables one to observe all of the anisotropic features without the need to reposition the specimen with respect to the magnetic field vector.

Another open question that remains to be answered is whether or not the orthorhombic phase is preserved in magnetic fields higher than 40 kOe. Our temperature-dependent measurements in several magnetic fields indicate that the hexagonal-orthorhombic transition with a change of slope of the *c*-lattice parameter still exists around 160 K in magnetic

fields above 20 kOe. Thus, assuming that the FM phase has the minimum energy in a distorted orthorhombic lattice and the PM phase maintains hexagonal type of crystal structure, the distortion should be preserved as long as Dy undergoes a transition to the ferromagnetic state.

CONCLUSIONS

The x-ray powder diffraction study of Dy was performed in the temperature interval from 5 to 300 K and in the range of magnetic fields from 0 to 40 kOe. The measurements confirm the complicated nature of magnetic-field–temperature phase relationships in the elemental Dy and agree well with the previously reported *H-T* magnetic diagrams.[4,6,7,14,15] We find that the ferromagnetic structure is only supported by the orthorhombic crystal structure, whereas helix, fan, and PM magnetic structures are stable in the hexagonal lattice. The hexagonal-orthorhombic distortion and the pronounced anomaly in the *c*-lattice parameter are coupled with AFM-FM transition at temperatures between 90 and 135 K. At temperatures above 135 K, the structural measurements show that these two phenomena are no longer coupled: the steps along the *c* axis do not correspond to the orthorhombic distortion and the latter becomes a second-order phase transition. The first-order phase transition corresponds to the helix transformation into either FM or fan phases below 170 K. The origins of a strong, field-independent heat-capacity peak around 90 K require further investigations.

ACKNOWLEDGMENTS

This work was supported by the Office of Basic Energy Sciences, Materials Sciences, Division of the U. S. Department of Energy under Contract No. DE-AC02-07CH11358 with Iowa State University.

*Present address: Physics Department, Purdue University, West Lafayette, Indiana, 47907-2036, USA.
†vitkp@ameslab.gov

[1] J. Jensen and A. R. Mackintosh, *Rare Earth Magnetism: Structure and Excitations* (Clarendon Press, Oxford, 1991), p. 403.
[2] F. J. Darnell and E. P. Moore, J. Appl. Phys. **34**, 1337 (1963).
[3] F. J. Darnell, Phys. Rev. **130**, 1825 (1963).
[4] R. Hertz and H. Kronmüller, J. Magn. Magn. Mater. **9**, 273 (1978).
[5] V. V. Vorob'ev, M. Ya. Krupotkin, and V. A. Finkel, Sov. Phys. JETP **61**, 1056 (1985).
[6] T. Izawa, K. Tajima, Y. Yamamoto, M. Fujii, O. Fujimaru, and Y. Shinoda, J. Phys. Soc. Jpn. **65**, 2640 (1996).
[7] A. S. Chernyshov, A. O. Tsokol, A. M. Tishin, K. A. Gschneidner, Jr., and V. K. Pecharsky, Phys. Rev. B **71**, 184410 (2005).
[8] S. A. Nikitin, A. S. Andreenko, and V. A. Pronin, Fiz. Tverd. Tela (Leningrad) **21**, 2808 (1979).
[9] A. M. Tishin and O. P. Martynenko, *Physics of Rare Earth Metals in the Vicinity of Magnetic Phase Transitions* (Nauka, Moscow, 1995), p. 336.
[10] A. E. Clark, B. F. DeSavage, and R. Bozorth, Phys. Rev. **138**, A216 (1965).
[11] Y. Kida, K. Tajima, Y. Shinoda, K. Hayashi, and H. Ohsumi, J. Phys. Soc. Jpn. **68**, 650 (1999).
[12] V. A. Finkel and B. C. Belovol, Sov. Phys. JETP **30**, 424 (1970).
[13] R. D. Greenough, G. N. Blackie, and S. B. Palmer, J. Phys. C **14**, 9 (1981).
[14] M. T. Alkhafaji and Naushad Ali, J. Alloys Compd. **250**, 659 (1997).
[15] A. V. Andrianov, Yu. P. Gaidukov, A. N. Vasil'ev, and E. Fawcett, J. Magn. Magn. Mater. **97**, 246 (1991).
[16] H. U. Astrom and G. Benediktson, J. Phys. F: Met. Phys. **18**, 2113 (1988).
[17] B. Coqblin, *The Electronic Structure of Rare-Earth Metals and Alloys: The Magnetic Heavy Rare-Earth's* (Academic, London, 1997).
[18] N. Wakabayashi, J. W. Cable, and J. L. Robertson, Physica B **241-243**, 517 (1998).
[19] Materials Preparation Center, Ames Laboratory of U.S. DOE, Ames, IA, USA, www.mpc.ameslab.gov
[20] A. P. Holm, V. K. Pecharsky, K. A. Gschneidner, Jr., R. Rink, and M. N. Jirmanus, Rev. Sci. Instrum. **75**, 1081 (2004).
[21] A. C. Larson and R. B. Von Dreele, Los Alamos National Laboratory Report LAUR 86-748, 2005 (unpublished).
[22] B. H. Toby, J. Appl. Crystallogr. **34**, 210 (2001).